Use of the perfect electric conductor boundary conditions to discretize a diffractor in FDTD/PML environment

C. Calderón-Ramón[a], J. F. Gómez-Aguilar[b], M. Rodríguez-Achach[c], L. J. Morales- Mendoza[a], J. R. Laguna-Camacho[a],
M. Benavides-Cruz[a], M. I. Cruz-Orduna [a], M. González-Lee[a], H. Pérez-Meana[d], M. Enciso-Aguilar[e],
R. Chávez-Pérez[f], and H. Martínez-García[a]
[a] Facultad de Ingeniería Mecánica y Eléctrica-
Facultad de Ingeniería Electrónica y Comunicaciones de la Universidad Veracruzana,
Venustiano Carranza s/n, Poza Rica Ver. México.
[b]Centro Nacional de Investigación y Desarrollo Tecnológico, Tecnológico Nacional de México,
Interior Internado Palmira S/N, Col. Palmira, Cuernavaca, Morelos, México.
[c]Facultad de Física, Universidad Veracruzana, Xalapa Ver. México.
[d]Escuela Superior de Ingeniería Mecánica y Eléctrica Culhuacán,
Av. Santa Ana 1000, Col. San Francisco Culhuacán, I.P.N, México D.F.
[e]Escuela Superior de Ingeniería Mecánica y Eléctrica Zacatenco,
Depto. de Telecomunicaciones,UPALM Edif. Z-4
[f] Centro de Investigación Científica y de Educación Superior de Ensenada, Ensenada B.C. México.

In this paper we present a computational electromagnetic simulation of a multiform diffractor placed at the center of an antenna array. Our approach is to solve Maxwell's differential equations with a discrete space-time formulation, using the Finite Difference Time Domain (FDTD) method. The Perfectly Matched Layers (PML) method is used as an absorbing boundary condition, to prevent further spread of the electromagnetic wave to the outside of the calculation region. The Perfect Electric Conductor (PEC) boundary conditions are used to represent the periphery of the region and the diffractor. The system consists of an antenna array of 20 elements: a transmission antenna (TX1) which feeds a Gaussian pulse with center frequency of 7.5 GHz, and 19 reception antennas (RX1 to RX19), which serve as sensors. The diffractor is discretized for integration into the environment FDTD, and two case studies are presented according to their geometric shape: square and circular diffractor. In this work, the goal is to determine the Maxwell's equations, analyze all the zones that form the diffractor and plug them in the computational algorithm in Matlab. We show the equations for each case and obtain the electromagnetic parameters of the system: electric fields, magnetic fields, and reflected power, sensed by the RX's.

Keywords: Conductor electric perfect conditions (PEC); finite difference time domain method (FDTD); perfectly matched layers (PML); antenna array; diffractor.

En este artículo se describe el uso de las condiciones de Conductor Eléctrico Perfecto (PEC), para modelar un difractor multiforme colocado en el centro de un arreglo de antenas. La estrategia se basa en resolver las ecuaciones diferenciales de Maxwell con una formulación discreta espacio-temporal, mediante el método de Diferencias Finitas en el Dominio del Tiempo (FDTD), el método de Capas Perfectamente Acopladas (PML), se utiliza como condición de frontera absorbente al evitar que la onda electromagnética continúe propagándose hacia el exterior de la región de cálculo, las condiciones de frontera PEC son utilizadas para representar la periferia de dicha región y el difractor. El sistema consiste en un arreglo de antenas, formado por 20 elementos: una antena de Transmisión (TX1) la cual alimenta un pulso gaussiano a una frecuencia central de 7.5 GHz y 19 antenas Receptoras (RX1 a RX19), que funcionan como sensores. El difractor es discretizado para su integración en el ambiente FDTD, se presentan dos casos de estudio, de acuerdo a su forma geométrica: difractor cuadrado y circular. Se presentan las ecuaciones correspondientes para cada caso, como resultado obtenemos los parámetros electromagnéticos del sistema: campos eléctrico, campos magnéticos, potencia reflejada, sensados por las RX.

Descriptores: Conductor eléctrico perfecto (PEC). Método de diferencias finitas en el dominio del tiempo (FDTD); capas perfectamente acopladas (PML); arreglo de antenas; difractor.

1. Introduction

Using Maxwell's equations, we can in principle determine the exact value of the electric and / or magnetic fields at any point in space or vacuum, when an electromagnetic wave impinges on an arbitrary structure. Analytical solutions of electromagnetic field scattering can be obtained using boundary conditions and separation of variables to solve simple shapes; however, for arbitrary geometries, the determination of the resulting fields it is only possible using computational methods.

The methods for numerically solving Maxwell's equations using FDTD [1, 8, 9, 11, 15] have been developed in the last decade. Determination of the required boundary conditions in FDTD can be done with the method of Finite Differences of Mur [2, 12], the Perfectly Matched Layer (PML) method of Berenger [4,16,17], or the model unidirectional wave equation of Engquist-Majda [3].

The computational electromagnetic tools used in this work are the FDTD and PML methods. Our system consists of an electromagnetic wave in vacuum, propagating into a circular array of 20 antennas. In the center of the array there is a diffractor that meets the PEC boundary conditions, which are expressed by a set of equations to discretize it in square and circular geometries. The equations are inserted in the computational algorithm for electromagnetic analysis. The emphasis of this article is the description of the PEC boundary conditions implemented to discretize the diffractor.

2. FDTD/PML environment

Formulation of the discrete Maxwell's equations is performed using the FDTD method [10, 14]. In order to solve them, an iterative process develops over time, this is well detailed in the literature as the PML [13] boundary conditions. Absorption processes are not addressed in this work.

We consider a two-dimensional system with a signal propagating in the "xy" plane, with a transverse component Hz, therefore the fields propagate in the transverse magnetic mode. This implies that the Hx, Hy and Ez components are zero, Ex and Ey are different from zero and there are no magnetic currents. The Maxwell's equations for the two-dimensional TM mode are:

$$\frac{\partial}{\partial t} H_z = -\frac{1}{\mu}\left(\frac{\partial}{\partial x} E_y - \frac{\partial}{\partial y} E_x\right) - \frac{\sigma^*}{\mu} H_z \quad (1)$$

$$\frac{\partial}{\partial t} E_x = \frac{1}{\varepsilon}\left(\frac{\partial}{\partial y} H_z\right) - \frac{1}{\varepsilon} J_{sx} - \frac{\sigma}{\varepsilon} E_x \quad (2)$$

$$\frac{\partial}{\partial t} E_y = -\frac{1}{\varepsilon}\left(\frac{\partial}{\partial x} H_z\right) - \frac{1}{\varepsilon} J_{sy} - \frac{\sigma}{\varepsilon} E_y \quad (3)$$

Where Hz is the transversal component of the magnetic field A/m; Ex, Ey are the components of the electric field in V/m; μ is the permeability in H/m; ε is the electric permitivity in F/m; σ is the electric conductivity in S/m and σ^* is the magnetic conductivity.

We use a finite differences method centered in space and time. In the following equations, we can see that there is not explicit dependence on time, this is because the time domain is implicit in the evolution of the computer simulation.

In Eq. (2) and Eq. (3), Jsx and Jsy represent the components of the electric current density in A/m.

The FDTD equations are:
a) Hz component:

$$Hz_{(i,j)} = \frac{\left(1-\frac{\sigma^*\Delta t}{2\mu}\right)}{\left(1+\frac{\sigma^*\Delta t}{2\mu}\right)} Hz_{(i,j)}$$

$$-\frac{\Delta t}{\mu\left(1+\frac{\sigma^*\Delta t}{2\mu}\right)}\left[\frac{E y_{(i+1,j)} - E y_{(i,j)}}{\Delta x}\right]$$

$$-\frac{\Delta t}{\mu\left(1+\frac{\sigma^*\Delta t}{2\mu}\right)}\left[\frac{E x_{(i,j+1)} - E x_{(i,j)}}{\Delta y}\right] \quad (4)$$

b) Ex component:

$$Ex^{n+\frac{1}{2}}_{(i,j+\frac{1}{2})} = Ex^{n-\frac{1}{2}}_{(i,j+\frac{1}{2})} \frac{\left(1-\frac{\sigma^*\Delta t}{2\varepsilon}\right)}{\left(1+\frac{\sigma^*\Delta t}{2\varepsilon}\right)}$$

$$+\frac{\Delta t}{\varepsilon\Delta y\left(1+\frac{\sigma\Delta t}{2\varepsilon}\right)}\left[Hz^n_{(i,j+1)} - Hz^n_{(i,j)}\right]$$

$$-\frac{\Delta t}{2\varepsilon\left(1+\frac{\sigma\Delta t}{2\varepsilon}\right)}\left[\frac{Jsx^{n+\frac{1}{2}}_{(i,j+\frac{1}{2})} + Jsx^{n-\frac{1}{2}}_{(i,j+\frac{1}{2})}}{2}\right] \quad (5)$$

c) Ey component:

$$Ey^{n+\frac{1}{2}}_{(i-\frac{1}{2},j+1)} = Ey^{n-\frac{1}{2}}_{(i-\frac{1}{2},j+1)} \frac{\left(1-\frac{\sigma^*\Delta t}{2\varepsilon}\right)}{\left(1+\frac{\sigma^*\Delta t}{2\varepsilon}\right)}$$

$$+\frac{\Delta t}{\varepsilon\Delta x\left(1+\frac{\sigma\Delta t}{2\varepsilon}\right)}\frac{\left[Hz^n_{(i,j+1)} - Hz^n_{(i-1,j+1)}\right]}{\Delta x}$$

$$-\frac{\Delta t}{2\varepsilon\left(1+\frac{\sigma\Delta t}{2\varepsilon}\right)}\left[\frac{Jsy^{n+\frac{1}{2}}_{(i-\frac{1}{2},j+1)} + Jsx^{n-\frac{1}{2}}_{(i-\frac{1}{2},j+1)}}{2}\right] \quad (6)$$

In the PML implementation of the above FDTD equations, we first need to decompose the transversal component Hz in the "x" and "y" projections, in such a way that $Hz = Hzx + Hzy$. In the Hzx projections we consider the variation of Ey with respect to "x", and similarly in the Hzy projection we consider the variation of Ex with respect to "y". Jsx and Jsy are null since there are not electric charges in the system, so they are not present in Eq. (5) and Eq. (6).

The Hz components are:

$$Hzx_{(i,j)} = \frac{\left(1-\frac{\sigma^*_x\Delta t}{2\mu}\right)}{\left(1+\frac{\sigma^*_x\Delta t}{2\mu}\right)} Hzx_{(i,j)}$$

$$-\frac{\Delta t}{\mu\left(1+\frac{\sigma^*_x\Delta t}{2\mu}\right)}\left[\frac{E y_{(i+1,j)} - E y_{(i,j)}}{\Delta x}\right] \quad (7)$$

$$Hzy_{(i,j)} = \frac{\left(1-\frac{\sigma^*_y\Delta t}{2\mu}\right)}{\left(1+\frac{\sigma^*_y\Delta t}{2\mu}\right)} Hzy_{(i,j)}$$

$$-\frac{\Delta t}{\mu\left(1+\frac{\sigma^*_y\Delta t}{2\mu}\right)}\left[\frac{E y_{(i,j+1)} - E y_{(i,j)}}{\Delta y}\right] \quad (8)$$

The complete PML implementation is done following the works in [5–7] where the Berenger method [4, 17] with some improvements are used.
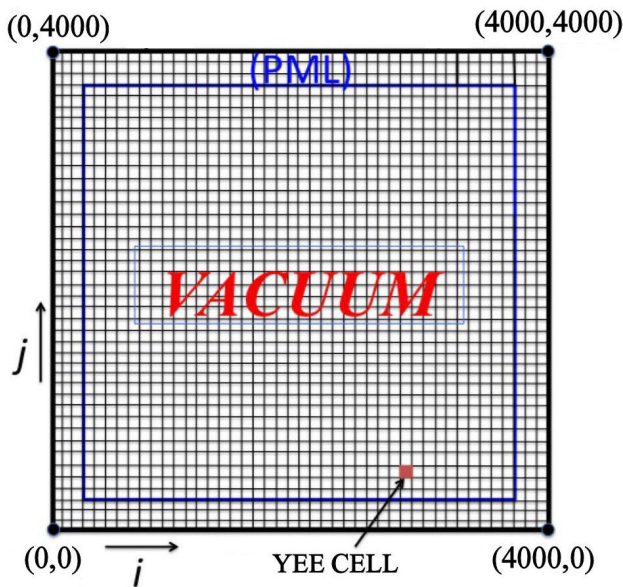
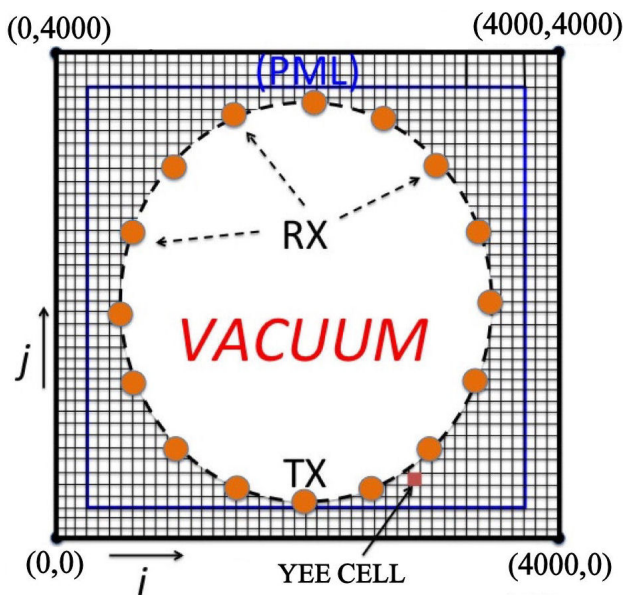FIGURE 1. Calculation region in FDTD/PML environment.

FIGURE 2. Array with one antenna TX and 19 antennas RX.

3.   Calculation Region

The region is shown in Fig. 1, where we can see the free space or vacuum part and the absorbing or PML region. Several regions have been simulated, but in this work we show two particular cases: one case of $1800i$ by $1800j$, equivalent to 3,240,000 and the second of $4000i$ by $4000j$ equivalent to 16,000,000 Yee cells, respectively. This is show in Fig. 1, where we see the absorbing or PML region, the Yee cells and the region of free space or vacuum.

The system parameters are:

$$\lambda = \frac{c}{f} = \frac{3 \times 10^8}{7.5 \times 10^9} = 0.04 m \qquad (9)$$

Where λ is the wavelength (m), f is the frequency (Hz), c is the speed of light (m/s).

Each Yee cell is two-dimensional and each of the Δx y Δy are calculated from the Courant condition [1] and are equivalent to:

$$\Delta = \Delta x = \Delta y = \frac{\lambda}{200} = \frac{0.04}{200} = 0.0002 m \qquad (10)$$

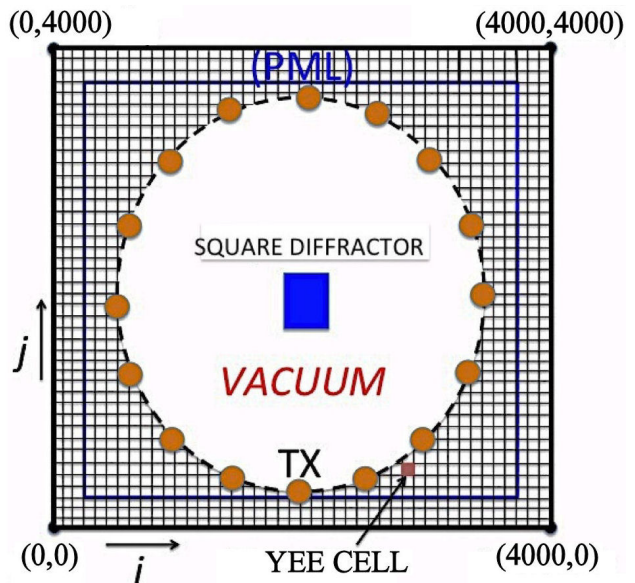Where Δ is the length of a Yee cell (m). Δt is the time step (s), equal to:

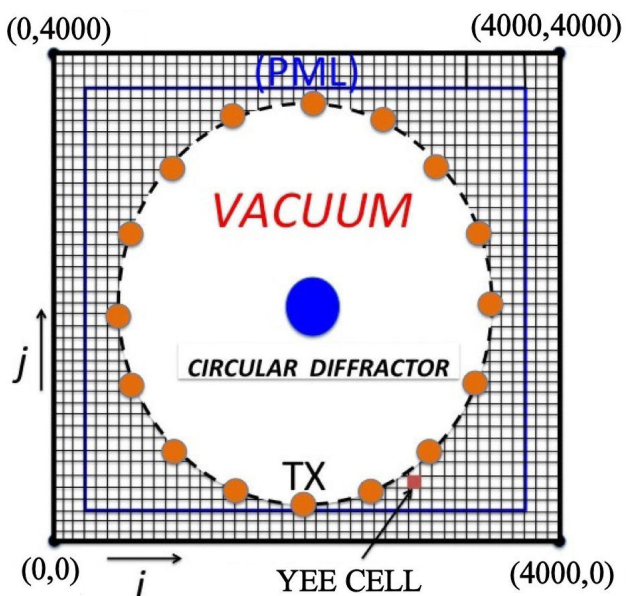FIGURE 3. Antenna array with a square diffractor inside.

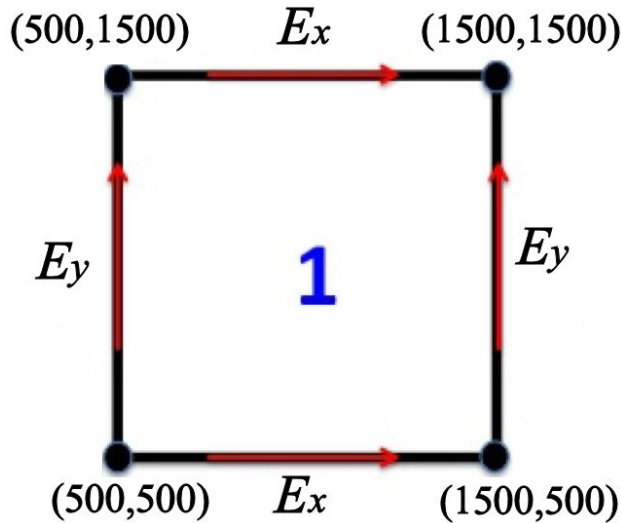FIGURE 4. Antenna array with a circular diffractor inside.

FIGURE 5. Discretization of square diffractor, zone 1.

$$\Delta t = \frac{\Delta}{2c} = \frac{0.0002}{2\,(3 \times 10^8)} = 0.33 \times 10^{-12} \qquad (11)$$

T is the period (s) :

$$T = \frac{1}{f} = \frac{1}{7.5 \times 10^9} = 1.33 \times 10^{-10} \qquad (12)$$

The antenna array diameter is equal to 1000 cells (Fig. 2), where the TX antenna transmits a Gaussian pulse of 7.5 GHz with a 6 to 9 GHz band width. The remaining reception antennas RX1 - RX19 are spaced 18 degrees and they are used as sensors to measure the electromagnetic parameters of the system.

The diffractor is placed in the center of the array, and we consider two geometries: square (Fig. 3) and circular (Fig. 4).
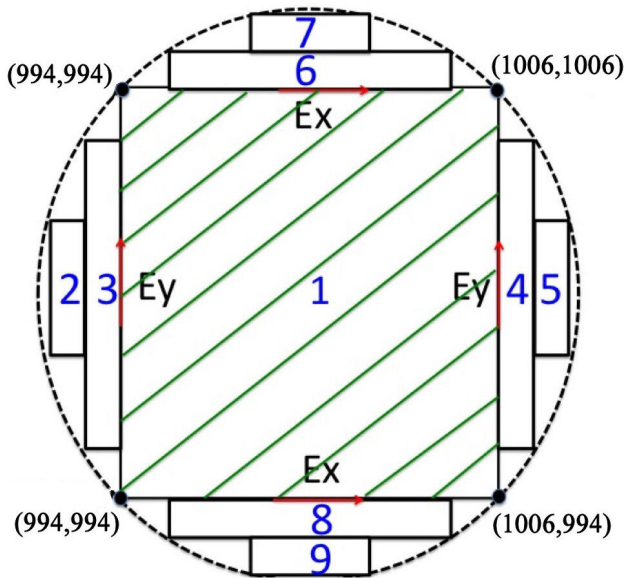

FIGURE 6. Discretization of a circular diffractor with 9 zones.

4. Perfect Electric Conductor (PEC) Boundary Conditions

Some considerations to establish the boundary conditions of a diffractor in vacuum are:

1. There are no charges or electric fields at any point within the conductor.

2. According to Gauss's law, the electric flux density has a direction normal to the surface and is equal to the charge density, then: $D_N = \rho s$.

3. The external electric field is decomposed into two components: a tangential (E_t) and a normal one (E_N), $E = E_t + E_N$.

4. The normal component of the magnetic field is zero, $H_N = 0$.

5. The tangential component of the electric field is zero, $E_t = 0$.

6. Knowing that $D = \varepsilon E$ and if $Et = 0$, then the tangential flux density is also zero, $D_t = 0$.

7. In relation to the external electric field with electric flux density we have:
$D_N = \varepsilon_0 E_N = \rho s$, then the electric field is normal to the surface of the conductor.

4.1. Square Diffractor

These equations are implemented in the computational algorithm in Matlab. The Fig. 5 shows the coordinates used for discretization.

The Table I shows the discretization equations of zone 1 of the square diffractor, where:

- Bottom: The tangential component of the electric field Ex is zero, from $500i$ cell to $1500i$ cell, in $500j$.

- Top: The tangential component of the electric field Ex is zero, from $500i$ to $1500i$ cell in $1500j$.

- Left: The tangential component of the electric field Ey is zero, from $500j$ to $1500j$, in $500i$.

- Right: The tangential component of the electric field Ey is zero, from $500j$ to $1500j$ in $1500i$.

TABLE I. Boundary Condition Equations for a square diffractor, zone 1.

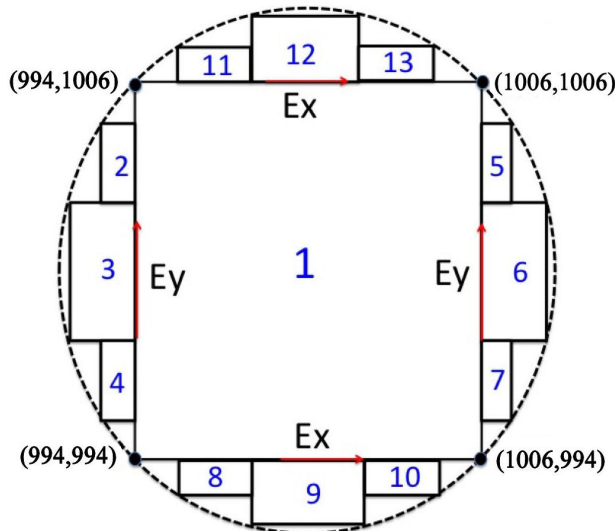| ZONE 1: Square diffractor	PEC EQUATIONS (Yee Cell)
Bottom Side	$Ex(500{:}1500,500){=}0$
Top Side	$Ex(500{:}1500,1500){=}0$
Left Side	$Ey(500,500{:}1500){=}0$
Rigth Side	$Ey(1500,500{:}1500){=}0$

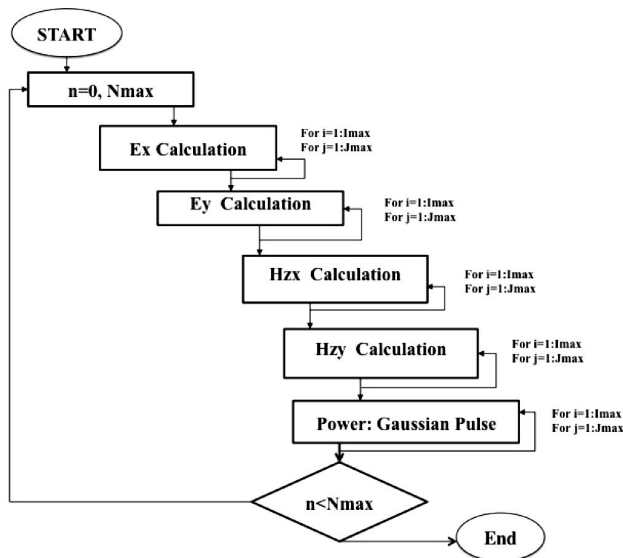FIGURE 7. Discretization of a circular diffractor with 13 zones.

FIGURE 8. Flow chart of the FDTD/ PML.

4.2. Circular Diffractor

For our next case of study, the diffractor is discretized in circular form. The FDTD method needs the regions to be represented in a simple geometric form. This is done with a set of 9 zones or with a set of 13 zones.

The steps for obtaining the relevant PEC equations are:

1. Define the geometric zones needed to form the circle, this is based on squares or rectangles.

2. Define the Ex and Ey components for each zone.

3. Define the start and end cells of each zone.

4. Set the equations that meet the boundary conditions of the perfect electrical conductor.

5. Implement these equations in the computational algorithm.

TABLE II. Boundary Condition Equations for a circular diffractor, zone 1.

ZONE 1: Circular diffractor	PEC EQUATIONS Yee Cell
Bottom Side	$Ex(994{:}1006, 994\,)=0$
Top Side	$Ex(994{:}1006,1006)=0$
Left Side	$Ey(994,994{:}1006)=0$
Rigth Side	$Ey(1006,994{:}1006)=0$

Example: Discretization of zone 1 (Fig. 6), where the position of the Yee cells can be seen. The total circle consists of 9 zones and the PEC Boundary Condition equations are given in Table II.

With the use of more zones, the circular region can be better defined, as in Fig. 7, where the discretization is represented by 13 zones. However, there is an increase in complexity obtaining the equations and their implementation in the algorithm. When done manually, this involves a lot of patience and care to avoid errors in the simulation.

Example: Discretization of zone 1 of the Fig. 7 shows the exact position in terms of Yee cells, where the total circle consists of 13 zones.

The flow chart of the whole computational implementation of the FDTD/PML algorithm used in this work is shown in Fig. 8:

5. Numerical Results

The results obtained from the program runs can be seen directly in the Matlab graphical interface. The initial calculation region is composed of 1800 by 1800 Yee cells. We must ensure the robustness of the algorithm, first of all, that there
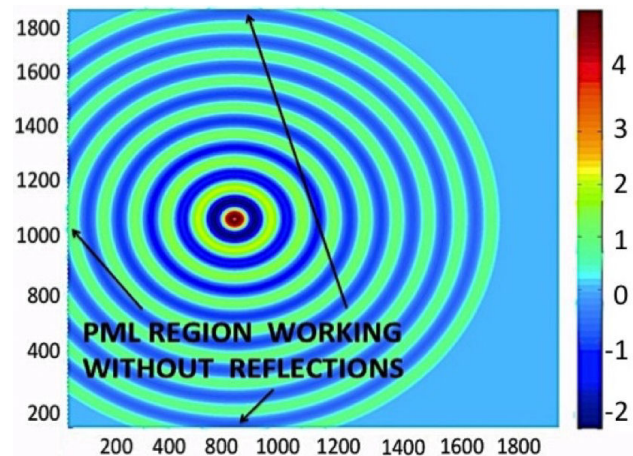

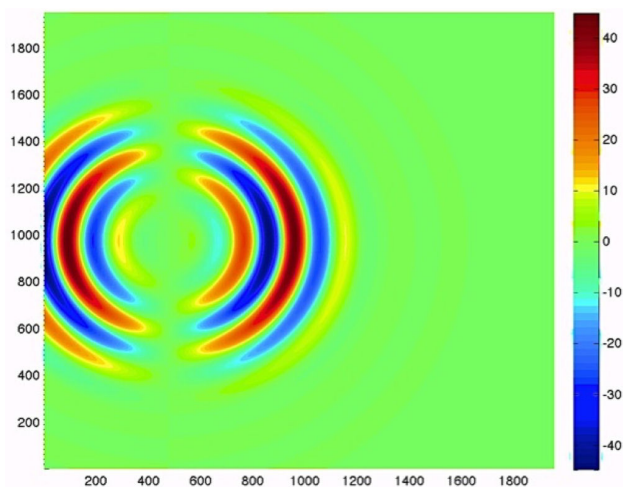FIGURE 9. Periphery without spurious reflections, Electric field in V/m.
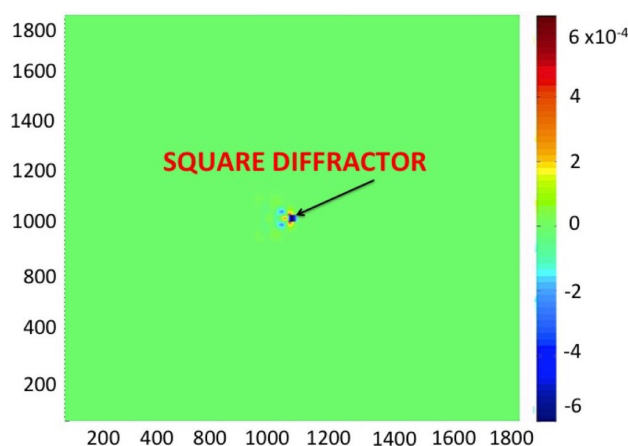
FIGURE 10. Gaussian pulse signal propagation.

FIGURE 12. Three collinear diffractors in vertical position.

FIGURE 11. Magnetic field resulting from the square diffractor, in A/m.

6. Conclusions

In this paper we have seen one of the significant advantages of the FDTD method, which is its flexibility to perform electromagnetic simulations. The PML was implemented to prevent, the propagation of the Gaussian pulse out of the region of calculation and therefore avoid spurious reflections at the periphery of the system. Using the perfect electrical conductor boundary conditions it is possible to simulate microwave devices, antennas, metals, dielectrics, etc.

We have presented a simple implementation of the FDTD and PML methods to simulate a circular array of "20" antennas with diffractors inside. To model them, it was necessary to discretize the diffractor by means of equations that meet the PEC boundary conditions for inclusion in the Matlab computational algorithm. The discretization of the diffractors was successfully realized as the numerical results show. The receiving antennas allows the measuring of the electromagnetic parameters, such as electric and magnetic fields, reflected power, among others.

The results obtained in this work show that we have a robust algorithm that permits the modelisation of an antenna array with diffractor inside in two geometric shapes, square and circular, also this technique was tested with three square diffractors. The calculation region was increased from $1800i$, $1800j$ to $4000i$ to $4000j$, Yee cells.

This study was motivated because of its possible application in the timely detection of breast cancer, in which the diffractors are replaced by a phantom (an object used as a substitute for malign tissue) that meets the electrical parameters of a breast tumor.

are not spurious reflections at the boundaries of the calculation region, that the implementation of the PML is correct, and the absorbing boundary conditions work correctly. As an example, in Fig. 9 we show the resulting electric field after the Gaussian pulse has been applied. Note that there are not spurious reflections at the boundaries, indicating that our algorithm is working correctly.

In Fig. 10 we can see the propagation of the Gaussian pulse signal, centered at 7.5 GHz.

In Fig. 11 we can see the magnetic field after the pulse signal has incided on the square diffractor. The values of this magnetic field are small compared with those in Fig. 9.

We now increase the region of calculation to 4000 by 4000 Yee cells and three diffractors have been placed in the array, as seen in Fig. 12. Here the electric field is in V/m.

Finally, we show the implementation of a circular diffractor in the center of the system. In Fig. 14 we show the electric field in V/m.
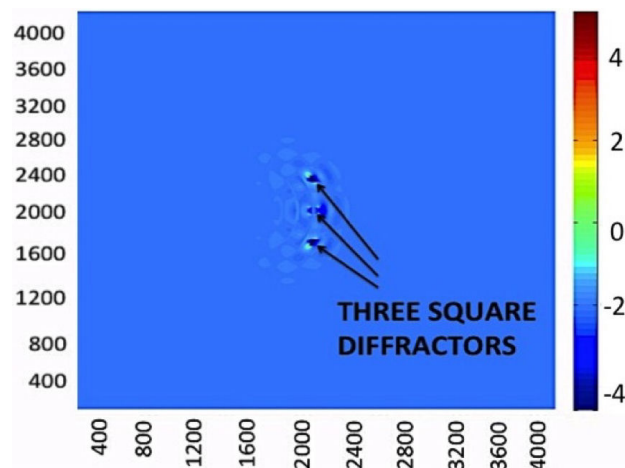
Acknowledgements

1. A. Taflove and S. Hagness, *Computational Electrodynamics: The Finite- Difference Time-Domain Method* 3rd edn. (Artech House, Norwood, MA, 2005).

2. G. Mur, *IEEE Trans. Electromagnetic Compatibility* **23** (1981) 377.

3. B. Engquist, A. Majda, *Math. of Comp*. **31** (1977) 629.

4. J. P. Berenger, *Journal of Computational Physics* **114** (1994) 185.

5. A. Benavides, M. Álvarez, M. Enciso, J. Sosa, *Analysis of polynomial and geometric conductivity profiles in PML layers: a comparison, Progress in Electromagnetics Research Symposium* PIER. (2010).

6. M. Benavides, M. Nieto, M. Enciso, J. Sosa, *Applied Mechanics and Materials* **15** (2009) 139.

7. M. Benavides *et al.*, *Rev. Mex. Fis* **57** (2011) 25-31.

8. K. S. Yee. *Numerical solution of initial boundary value problems involving Maxwell's equations in isotropic media, IEEE Transaction Antennas and Propagation* **AP-14** (1966) 302-307.

9. D.M. Sullivan, *IEEE Press Series on RF and Microwave technology* New York (2000).

10. A. Elsherbeni, V. Demir, *The Finite-Difference Time-Domain Method for Electromagnetics with MATLAB Simulations, SciTechPublishing Inc,* Raleigh N.C, USA, (2009), pp. 187-215.

11. M. Benavides-Cruz, doctoral thesis, SEPI-ESIME IPN, (2011).

12. C.Calderón-Ramón, doctoral thesis,SEPI-ESIME, IPN, (2015).

13. C. M. Calderón, H. M. Pérez, A. M. Benavides, L. J. Morales, *Desarrollo de un Arreglo Circular de Antenas utilizando herramientas de Electromagnetismo Computacional. Centro de Informacioón Tecnológica*, **25** (2014) 41-54.

14. M. Lopez, *Rev. Mex. Fis* **E52** (2006) 58-64.

15. A. M Benavides *et al.*, *Rev. Mex. Fis E*, **57** (2011) 25-31.

16. J. Berenger,*AntennasandPropagation,IEEETransactions* 44 (1996) 110-117.

17. J. Berenger, *Antennas and Propagation, IEEE Transactions* **47** (1999) 1497-1503.